November 30, 1994

Microtribological Characterization of Self Assembled and Langmuir-Blodgett Monolayers by Atomic and Friction Force Microscopy

Bharat Bhushan, Ashok V. Kulkarni and Vilas N. Koinkar

Computer Microtribology and Contamination Laboratory
Department of Mechanical Engineering
The Ohio State University
Columbus, OH 43210-1107, USA

Mathieu Boehm, Ludovic Odoni and Claude Martelet

Laboratoire de Physicochimie des Interfaces

Michel Belin

Laboratoire de Tribologie et Dynamique des Systemes
Ecole Centrale de Lyon
B.P. 163
69131 Ecully Cedex, France

ABSTRACT

Organized and dense monolayers were produced by chemical grafting of molecules and by Langmuir-Blodgett (L-B) deposition. Friction, wear and indentation of these films on a microscale have been studied using atomic force microscopy/friction force microscopy (AFM/FFM). For comparison, macroscale friction and wear measurements have also been made. Mechanisms of friction, wear and lubrication of chemical grafted and L-B films are discussed. These studies show that coefficient of friction, wear resistance, and nanoindentation properties of C_{18} double grafted films are superior to L-B films. It is concluded that chemical grafted films may be suitable for lubrication of microcomponents.

I. INTRODUCTION

Microelectromechanical Systems (MEMS) include microsensors, fine-polishing microactuators, microgrippers, micromotors, micropumps, gear trains, cranks, manipulators, nozzles and valves. These, a fraction of a millimeter in size, are being fabricated in laboratories around the world. Free standing polysilicon films are used for construction of MEMS (Howe, 1988, Fan et al., 1989; Tai and Muller, 1989). Because of large surface area to volume ratio in the MEMS, the electrostatic and friction forces become predominant over inertial and gravitational forces. Therefore, friction in MEMS becomes a more stringent problem than that in macrosystems. A number of attempts have been made to measure friction and wear of MEMS (Gabriel et al., 1990; Fujita, 1992). Hard coating (such as silicon nitride and diamond-like carbon) and solid and liquid lubricants have been tried to minimize friction and wear of MEMS (Tai and Muller, 1989; Suzuki et al., 1991; Jaffrezic-Renault and Martelet, 1992; Zarrad et al., 1993).

Owing to the microsize of the MEMS components, classical lubrication approach of the use of freely supported multimolecular layers is not most desirable. A preferred method of lubrication is by the deposition of organized and dense molecular-scale layers of preferably long-chain molecules as they have been shown to be superior lubricants on a macro scale (Bowden and Tabor, 1950; Suzuki et al., 1988; Ando et al., 1989; Ruhe et al., 1993; Zarrad et al., 1993). Common methods to produce monolayers and thin films (Ulman, 1991) are the Langmuir - Blodgett (L-B) deposition (Roberts, 1990; Zasadzinski et al., 1994) and self-assembled films by chemical grafting of molecules (Serpinet et al., 1980; Szabo et al., 1984; Jaffrezic-Renault and Martelet, 1992). The L-B technique can only be used on flat geometry whereas the chemical grafting can be accomplished over 3-D complex surfaces. The L-B films are bonded to the substrate by weak van der Waals attraction. Whereas, the grafting process forms a direct covalently-bonded dense films of long chain molecules. Flexibility of choosing the alkyl chain length, functional terminal

group and cross linking enables the adaptability of grafting process to many lubrication situations.

Macroscale friction and wear measurements of films produced by grafting of long-chain molecules onto hydroxylated silica surfaces (Zarrad et al., 1993) and of L-B films (Ando et al., 1989) have shown that these films improve the tribological performance of silica surfaces. Micro-scale measurements at ultra low loads are needed to assess the lubrication behavior of these films for MEMS. Atomic force microscopy (AFM) and friction force microscopy (FFM) are suitable techniques to study thin organic films on a microscale (Bhushan, 1995). AFM has been used to image and detect defects in such films (Hansma et al., 1991; Viswanathan et al., 1992; O'Shea et al., 1993; Overney et al., 1993; Pan et al., 1993; Schwartz et al., 1993; Liu and Salmeron, 1994) and FFM has been used to make micro-scale friction measurements (Meyer et al., 1992; O'Shea et al., 1993; Overney et al., 1994). Objective of this research is to make micro-scale friction and wear measurements which better simulate the contacts in a MEMS. Results of this research are reported in this paper.

II. EXPERIMENTAL DETAILS

II.1 Preparation of Films

Octodecyl (C_{18}) grafted films were condensed on a Si (100) p-type wafer of low doping density ($10^{21}m^{-3}$) from CSEM (Neuchatel, Switzerland) covered by a thermally-grown SiO_2 layer, Fig. 1. Thickness of the SiO_2 layer was measured by ellipsometry (rotating analyzer ellipsometry) and was 65-75 nm. After cleaning in ultra pure water for about 10 minutes, hydroxylation (activation process) and drying at 140°C in vacuum (0.4 Pa) for 2 hours, the organic film alkyl dimethyl (dimethyl) aminosilane was condensed. This grafting reaction took place in dry nitrogen flow at 140°C for 48 hours (Serpinet et al., 1980; Szabo et al., 1984; Duvault et al., 1990). For the benefit of tribology readers

who may not be familiar with chemical grafting process, for completeness a summary of the process used in this study follows.

The hydroxylation of silica was performed through a sulfochromic treatment. The sample was dipped in a solution consisting of 100 ml concentrated H_2SO_4, 5 ml water and 2 g potassium bichromate for 3 to 15 minutes. The sample was then rinsed with flowing pure water:

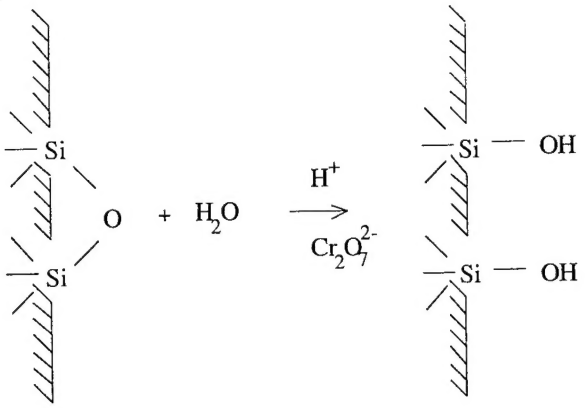

(1)

Duvault et al. (1990) have demonstrated this treatment to act as a good chemical cleaner of the silica, preserving its structure and rendering the surface hydrophilic. It allows a high density of surface silanol groups which can be used for the coupling of the reactive species.

Next we describe the procedure to prepare reactive monofunctional alkyl dimethyl (dimethyl) aminosilane required for grafting. The first step is to obtain the alkyl dimethylchlorosilane by hydrosilanization of the 1-alkene with dimethylchlorosilane in the presence of chloroplatinic acid:

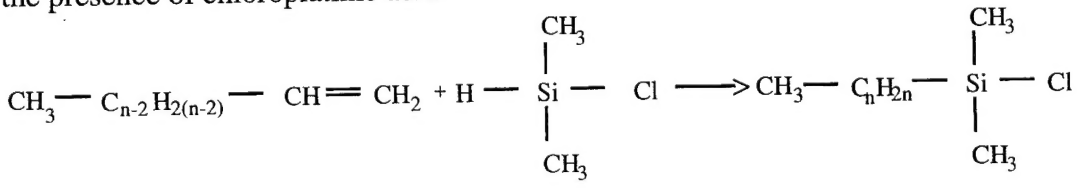

(2)

This reaction is carried out under nitrogen flow. The reagent vapour is condensed under isopropanol flowing at -10°C. After 18 hours, the total disappearance of 1-alkene is checked by IR-spectroscopy. Chlorosilane is distilled in vacuum. The amination reaction is carried out to produce the alkyl dimethyl (dimethyl)

aminosilane:

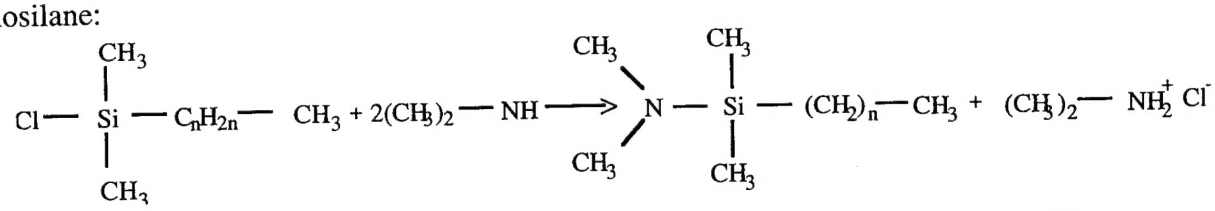

(3)

This reaction is performed at room temperature in hexane, under a nitrogen flow. A stream of isopropanol antifreeze at -30°C flows through the cooler because of the reagent's volatility. After the distillation of hexane, dimethyl ammonium chloride is separated by filtration and then aminosilane is distilled in the vacuum.

In order to produce the grafted film on the hydroxylated SiO_2/Si wafer, it was dried at 140°C in vacuum for 2 hours. The SiO_2 surface was coated with aminosilane, in a 2 vol.% solution of silane in isopentane at -30°C, in vacuum for 2 hours. After the isopentane was removed completely, the grafting reaction took place at 140°C in dry nitrogen for 48 hours. This grafting reaction is:

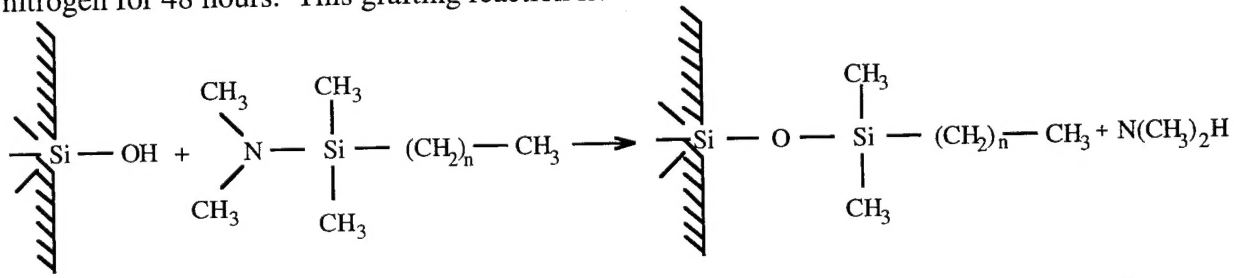

(4)

The excess of silane was washed off with tetrahydrofuran. To obtain high coverage, it is necessary to repeat the silanizing treatment once and these films are referred to as double grafted films. Before the measurements, the grafted samples were cleaned in Xylene at 100°C for 10 minutes. They were rinsed in double deionized water and then dried under nitrogen flow. Octodecyl (C_{18}) and commonly used docosyl (C_{22}) films are produced by using different structures of aminosilanes. Thicknesses of octodecyl films (n=17) measured using ellipsometry (rotating analyzer ellipsometer) were 2.8 nm.

The structure and composition of the L-B films and substrate used in this study are shown in Fig. 2. These films were prepared in the lab of Prof. Martin Caffrey. Following description is based on Wang et al. (1994). Film structure consisted of an octadecylthiol (ODT) coated gold sample (gold films thermally evaporated onto single-crystal silicon) on top of which a single, upper inverted bilayer of zinc arachidate (C_{20}, ZnA) was deposited by the L-B technique. After plasma cleaning the gold surface, it was immersed in 1 mM ODT in tetrahydrofuran (THF) and incubated at room temperature for 6 to 12 hours to complete the formation of a hydrophobic monolayer. The sample surface was rinsed extensively with THF to remove the excess ODT. L-B deposition was performed using KSV MiniTrough system (KSV Instruments, Riverside, CT) in a clean room at 23 to 25°C. In preparation for deposition of L-B films of ZnA, a subphase containing 0.1 mM $ZnCl_2$ in 1 mM $NaHCO_3$ buffer (pH=7.1) was used. After the arachidic acid was spread from a 1 mM solution in chloroform as above and compressed, a ZnA monolayer was formed at the air/subphase interface as a result of electrostatic binding of $Zn^{2}+$ to two arachidate carboxylate anions. The ZnA adlayers were prepared at deposition rate of 3.0 mm/min. and a surface pressure of 20 mN/m corresponding to an area of 0.4 nm^2 per ZnA. A transfer ratio of unity ($\pm$ 10%) was observed for depositions by monitoring the area loss of the film at the air/subphase interface per unit of substrate area passing through the interface. Thicknesses of the successive layers were determined using an ellipsometer (Model L116C, Gaertner Scientific Corp., Chicago, IL). The thicknesses of ODT, and ZnA bilayer were 2.2 nm and 6.6 nm respectively. For further details, see Wang et al. (1994).

We note that bonding of S (in the ODT film) to the substrate in the case of L-B films is about half as strong as that Si-O bond to the substrate in the case of grafted films, Table 1. Furthermore, the ODT film is weakly bonded to the ZnA bilayer by weak van der Waals attraction.

II.2 Description of AFM/FFM and Measurement Techniques

A modified commercial AFM was used to conduct studies of surface topography, friction and wear of self assembled and L-B films on a micro- to nanoscale. Topography, friction and nanowear measurements were made using microfabricated square pyramidal Si_3N_4 tip with a tip radius of about 30 nm (normal cantilever stiffness ~ 0.58 N/m) and at normal forces ranging from 10 nN to 200 nN. Intrinsic adhesive forces were included for calculation of total normal force. The sample was scanned under the tip with a typical scanning speed of 4 μm/s in the fast scan direction and 8 nm/s in the perpendicular direction for a 1 μm x 1 μm area. By making measurements at various normal loads, average value of coefficient of friction was obtained which can then be used to convert the 3-D friction force profile to the coefficient of friction profile. Thus, any directionality and local variation of friction can be measured. Surface topography and friction data can be measured simultaneously and local relationship between the two profiles can be established (Ruan and Bhushan, 1994; Bhushan, 1995). All measurements were made with the same tip. Whether the tip got contaminated or not was confirmed by first scanning the tip on a clean silicon sample and then measuring the adhesive force in the force calibration mode. Any increase in the adhesive force from a typical value for a clean tip indicated that the tip was contaminated and it needed to be replaced. The uncertainty associated with the average coefficient of friction was within ± 15%.

Single-crystal natural diamond tip was used for microwear measurements at relatively higher loads. The diamond tip is ground to the shape of a three-sided pyramid with an apex angle of 80° whose point is sharpened to a radius of about 100 nm. The tip is bonded with conductive epoxy to a gold-plated 304 stainless steel spring sheet (length = 20 mm, width = 0.2 mm, thickness = 20 to 60 μm) which acts as a cantilever. Typical normal force used for the micro wear studies ranged from 1 μN to 60 μN with a cantilever stiffness of about 25 N/m. For micro wear studies, an area of 1 μm x 1 μm was scanned with the scanning speed of 4 μm/s in the fast scan direction and 8 nm/s in

the slow scan direction. Sample surfaces were scanned before and after the wear to obtain the initial and final topography at a normal force of about 0.3 μN, over an area larger than the worn region to observe the wear scars. Additional wear may have occurred during these scans, but this wear is much smaller than that generated at higher normal force (>1 μN). To minimize additional wear, all images were captured during the first scanning cycle. All measurements were made using the same diamond tip. Periodically, the tip was scanned on a clean single-crystal silicon sample to clean it and to find out whether tip got contaminated. If subsequent measurements of adhesive force indicated any contamination, then the tip was cleaned by pressing the tip on a sponge soaked with isopropyl alcohol. Reproducibility in the wear rates was good (within ± 20%).

III. RESULTS AND DISCUSSION

III.1 Topographical and Friction Imaging

Surface topography and friction force images of L-B films and grafted films were recorded simultaneously over a region of 1 μm x 1 μm. The surface roughness and coefficient of friction values of the specimen studied are listed in Table 2. The normal load during imaging of the SiO_2 surface and the grafted films was 100 nN, whereas normal force used for Au/Si, ODT/Au/Si and ZnA/ODT/Au/Si was 40 nN because these films wore readily at higher loads. Figure 3 presents the gray scale plots of surface topography, surface slope and friction images of SiO_2 layer, C_{18} single grafted and C_{18} double grafted films. The SiO_2 layer has a roughness value of 0.21 nm rms. The single and double grafted C_{18} films have lower roughness value compared to the SiO_2 layer. The asperities (bright spots) as seen in the topographical images of the grafted films were noticeably less as compared to the SiO_2 layer. The grafted film surfaces appear to be homogenous and no holes could be seen after scanning over different regions. The grafted films consist of C_{18} molecules in the monolayer which are well oriented with the

alkyl chains being almost perpendicular to the surface with their functional group at the top. It is hence expected that the film surface be homogenous and devoid of high asperities. The only difference between the single and double grafted film is the density of the grafted alkyl chains on the SiO_2. Therefore the two surfaces show similar roughness values. The slope of the surface profile was taken along the sample sliding direction. No direct correlation between the surface profiles and the corresponding friction force profiles is observed in these figures. The high and low points on the roughness profiles do not correspond to the high and low points on the friction force profile respectively. Local changes in the friction force profile are attributed to the presence of microscopic defects and other local chemical changes.

The coefficient of friction values for the grafted specimens were obtained by making friction measurements at different normal forces in the range of 0-200 nN. Figure 4 shows the variation of the friction force as a function of normal force for SiO_2, C_{18} single grafted and C_{18} double grafted films. All three plots show a linear variation of friction force with normal force. The coefficient of friction of SiO_2 is 0.03 and is comparable to that reported by Bhushan and Koinkar (1994). The C_{18} single grafted film shows a friction value of 0.04 which is slightly higher than the SiO_2 layer, while the C_{18} double grafted film on the contrary shows a very low friction value of 0.018. Intercept of the friction force line with the normal force axis gives the intrinsic adhesive forces resulting form meniscus effect. The intrinsic force values obtained from these plots are comparable with those measured in force calibration mode.

The tribological performance of the grafted films depend on their properties such as the chain length of the alkyl molecules, the surface on which these molecules are grafted, the areal density (i.e. the density of the alkyl molecules) and method of preparation etc. (Duvault et al., 1990). The alkyl chains being flexible can dissipate mechanical energy from the shearing process (Ruhe et al., 1993). The chain-chain interaction to a large extent also governs the mechanical properties of these films. High

areal density leads to strong chain-chain interaction thereby improving the tribological performance. Since C_{18} single grafted film lacks in coverage density, it is expected that there must exist microscopic empty sites or patches, which are termed as defects or disorder in the film resulting in higher coefficient of friction. The C_{18} double grafted film has higher areal density and hence stronger chain-chain interaction leading to better tribological performance. Superior frictional behavior of double grafted films is consistent with the macro-scale measurements reported by Zarrad et al. (1993).

Figure 5 shows topographic, surface slope and the corresponding friction force images of Au/Si, ODT/Au/Si and ZnA/ODT/Au/Si. The imaging of both topography and friction force of these specimen were carried out over a 1 μm x 1 μm region at a normal force of 40 nN. The surface topography of gold film deposited on silicon revealed presence of particles. The surface roughness of Au film is 1.16 nm rms and coefficient of friction is about 0.04. The topography of ODT/Au/Si shows a relatively smooth surface with a surface roughness value of 0.92 nm rms which is less than the roughness value of Au surface. It is expected that the ODT layer forms a homogenous and a flat surface over the Au film, since it is known that these organic layer provide a high absorbtion to the solid substrate (Overney et al., 1993). Presence of any particles and high asperities in the topography of the ODT results from the Au film surface. The ODT layer consists of thiol molecules which are well organized structures, leading to a smoother surface and hence reduction in the surface roughness value. Coefficient of friction of the ODT/Au/Si layer is 0.03 comparable to single grafted C_{18} film. This can be attributed to the fact that the ODT layer has a short chain length measuring 2.2 nm, which do not give much protection for the shear forces. So even small loads can initiate wear of the film resulting in removal of the layers.

The topography of ZnA bilayer film shows a smooth surface with few bright and circular dark spots distributed over the region. The surface roughness is less compared to the Au and ODT surfaces. The friction image however, exhibits high friction points. The

circular holes in the surface profile correspond to the dark areas in the image. These holes are of the size of 10-100 nm and indicates that these films are not defect free. The appearance of holes in the film has also been reported by other authors (Viswanathan et al., 1992). Imaging of L-B films is possible only at extremely small applied loads as the film can be degraded or the molecules can be displaced by the sharp AFM tip. The surface slope again do not correlate well with the friction profiles except in the case of Au, where we notice resemblance between local variation in the surface slope and local variation in the friction. The ODT and ZnA friction images are very much dissimilar as compared to the surface slope which suggests that surface defects (and not topography) strongly affects the friction.

Figure 6 shows the variation of the friction force as a function of normal force for the Au/Si, ODT/Au/Si and ZnA/ODT/Au/Si specimens. The normal force was in the range of 10-200 nN. Since L-B films are quite fragile, the normal load was limited to 120 nN for measurement of coefficient of friction. The friction force for the Au, ODT/Au/Si and ZnA/ODT/Au/Si specimens changes linearly with the normal force. The gold film shows a coefficient of friction value about 0.04. The ODT and ZnA layer on the contrary show reduced friction value of 0.03. Except for the difference in the chain length, both ODT and ZnA films are organized molecular structures with the same functional end group which explains the similar friction value exhibited by these two films.

Topographic images of C_{18} double grafted film (2 nm x 2 nm) were obtained at normal force of 40 nN and 250 nN and the corresponding 2-D Fourier transform of images are shown in Fig. 7(a) and (b) respectively. The bright spots in the topographic image shows the hexagonal arrangement with nearest neighbour distance of 0.45 nm $\pm$ 0.05 nm. This value is comparable to that reported by Duvault et al. (1990) and Liu and Salmeron (1994). A slight structure transformation was observed between the normal forces of 40 nN and 250 nN. The critical normal force for the structural transformation also depends upon the tip radius.

III.2 Nanowear Studies

L-B films are fragile as compared to grafted films and wear readily. Therefore, wear studies on the L-B film were conducted at very small loads. The surface was scanned at 1 μm x 1 μm region at a constant normal force of 200 nN a few times with Si_3N_4 tip. The friction profiles after each cycle upto four cycles were recorded [Fig. 8(a)]. Figure 8 shows the friction image after the completion of one scan cycle. The image after first scan cycle depicts regions of a high friction where the removal of the L-B film has taken place. The organic molecules are displaced under the tip and the debris results into higher friction. After the second scan cycle, these high friction areas tend to move towards the edge of the scan region. After the third and fourth scan cycles, the bright areas moved to the far edges of the scan region. Repeated scan results in the wear of the L-B film. The friction profile after four scan cycles shows that the L-B film is removed completely and friction measured in this region is on the underlying ODT layer. The wear is first initiated at sites where earlier microscopic defects were present and the wear debris is transported further with each consequent scan. A topographic image after completion of four scan cycles recorded at a normal force of 40 nN over a region of 2 μm x 2 μm enclosing the wear area is shown in Figure 8(b). The central region of 1 μm x 1 μm shows the worn region with the debris at the left and right edges of the scan frame. The debris is collected at the edge of the worn region in the scanning direction of the tip. The fact that the debris can be seen as collected on the sides of the scan frame and is not scattered over the region suggests that the thiol molecules are laterally displaced by the tip during the scan. This behavior has also been observed by Overney et al. (1994). The debris in our case is seen to have collected in the form of two distinct steps. A 2-D section analysis reveals the height of the steps to be of approximately 6.5 nm which is same as the chain length of the ZnA bilayer. This results shows that with each scan a bilayer of the ZnA film is removed as a single structural unit

and deposited on the edge. Consequent scan leads to the build up of the debris with a typical step height comparable to the chain length. The exact nature of the transport of the debris is not fully understood. This result also indicates that the ZnA bilayer does not break up into smaller structural units under the action of the tip. Similar experiments were conducted on C_{18} single and double grafted films. No change in the surface profile was observed even after scanning for 10 cycles.

III.3 Micro Wear Studies

Wear studies on the grafted films and the corresponding SiO_2 substrate and L-B films and corresponding Au/Si and ODT/Au/Si substrates were performed using a three sided pyramidal diamond tip at loads ranging from 1 to 60 μN. An area of 1 μm x 1 μm was scanned at desired load for one cycle. To obtain the wear mark images, larger area of 2 μm x 2 μm was scanned at a smaller normal force about 0.3 μN. Wear depth was obtained by taking an average of the surface heights in the wear region. Figure 9 shows the plot of wear depth as a function of normal force after one cycle for SiO_2, C_{18} single and double grafted films . The SiO_2 specimen does not show any wear upto normal force of 15 μN. Wear mark is visible in C_{18} single grafted film at 10 μN normal force, while C_{18} double grafted film could not be scratched below a normal force of 25 μN. Wear depth in all the cases increased linearly with the normal force. In the case of Au/Si and ODT/Au/Si layer, a normal load of 2 μN was sufficient to cause wear. Even a small increase above the 2 μN normal force led to significant wear of the film. L-B films was removed at a normal force of 0.2 μN after one cycle. Representative wear mark profiles for all samples are shown in Fig. 10. The wear mark profile of ZnA after completion of four scan cycles is also shown in Fig. 10.

The results of wear depth as a function of number of cycles are shown in Fig. 9(b). For SiO_2, C_{18} single grafted and double grafted films a normal force of 25 μN was used while that for Au/Si and ODT/Au/Si a normal load of 2 μN was employed, and for

ZnA film lowest load of 0.2 μN was used. SiO_2 layer showed a good wear resistance behavior upto 30 cycles after which the wear increased linearly (Bhushan and Koinkar, 1994). The single grafted C_{18} film showed higher wear than SiO_2 with a maximum wear depth of 23 nm after 80 cycles . Higher wear in this film is attributed to the presence of microscopic defects which are abundant in this film. The areal density probably being less in this film leads to initiation of wear and hence increasingly more wear with each cycle . Owing to these reasons the friction of this film too showed higher value than the C_{18} double grafted film. The C_{18} double grafted film on the other hand shows improved wear resistance. The initial wear upto 40 cycles is very nominal, the wear depth being 2.4 nm, which is comparable to the chain length of C_{18} molecules. Once the C_{18} layer is removed wear depth increases linearly with increase in the normal force . After 80 cycles the wear depth is 13.5 nm which is the same observed for SiO_2 film. Surface profiles of the wear mark generated on C_{18} double grafted layer for a certain number of cycles are presented in Figure 11. After five cycles the wear depth is 0.4 nm, while after 30 cycles the depth is 2 nm. The wear of the film is not significant upto 40 cycles. After 40 cycles the wear depth increases sharply. The wear depth after 50 cycles was found to be 4.4 nm. This indicates that the C_{18} double grafted layer has been completely removed in the wear region of 1 μm x 1 μm after 40 cycles since the monolayer thickness is 3.2 nm. At the end of 80 cycles the wear depth of C_{18} double grafted film is 13.5 nm which is the same as observed in case of SiO_2. The Au/Si and ODT/Au/Si on the other hand exhibit higher wear even at small loads. The wear of Au and ODT shows similar wear profiles with the ODT showing more wear than the Au film. The wear depth after 60 cycles in the two cases was 17 and 20 nm respectively. ZnA film wore in one cycle at lower load of 0.2 μN. It can be seen from these plots that the C_{18} double grafted film shows higher wear resistance. The grafted layers are alkyl monolayers covalently bonded on silica surface, while ZnA film is formed by LB technique, wherein organized monolayers of amphiphilic molecules are transferred from air-water interface to the substrate

(Zasadzinski et al., 1994). Increased wear resistance observed in the grafted film is attributed to the fact that Si-O bond is more stable than Au-S bond. Further the ODT film is weakly bonded to the ZnA bilayer by the weak van der Waals attraction as a result of which it exhibits poor tribological performance.

III.4 Nanoindentation studies

The nanoindentation studies were performed on the single crystal silicon (100), C_{18} double grafted and ZnA films using atomic force microscope in the force calibration mode. The cantilever force versus sample traveling distance curves were obtained by moving the sample towards and away from the Si_3N_4 tip, the sample traveling distance and cantilever deflection were measured simultaneously. Force versus distance plots obtained for three different samples are shown in Fig. 12. The sample traveling direction is shown by arrows. Initially sample is farther away from the tip. As the sample comes in close proximity to the tip, the attractive forces between atoms on sample surface and tip becomes dominant and the cantilever bends towards the sample. Further pushing of the sample against the tip results into the linear deflection of cantilever with sample traveling distance. The cantilever deflection when the sample retraces its path is also recorded. During the retracing of the sample from tip, cantilever beam moves with the sample and remains in contact until the force on cantilever is higher than the adhesive force because of meniscus effects. The difference between the trace and retrace path is because of the hysteresis effect of PZT tube scanner used in the AFM for scanning the sample. Using this method it has been demonstrated by several researchers (Weisenhorn et al., 1992; Burnham et al., 1993) that the attractive and adhesive force between tip and sample can be measured.

For the solid/rigid sample, the cantilever deflection is equal to the sample traveling distance with the slope of 1.0 after tip to sample contact. The maximum normal force applied is about 18 nN. In this study we have used single-crystal silicon sample as

a rigid sample and calibrated the force versus distance curves as shown in Fig. 12(a), where a slope of 1.0 was observed. Figure 12(b) shows the force versus distance curve for the C_{18} double grafted film. This curve gives the slope of 1.0 and indicates that the grafted layer behaves like rigid surface. For the L-B film [Fig. 12(c)] we have obtained the slope of about 0.91 which clearly shows that the tip has indented into the film. Equal slope during unloading suggests that indentation is elastic and recovers during unloading. Indentability of the film suggest that these films are softer than C_{18} double grafted films. We have observed similar results during the nanowear tests, Fig. 8. We further studied systematically the indentation effect on L-B films. Figures 13(a) and (b) show the curves for L-B films obtained at normal forces of about 18 nN and 32.4 nN, respectively. Initially, we applied force of 18 nN and then increased upto the value of 32.4 nN for few seconds. In both cases slope obtained is about 0.95. It is interesting to note that after bringing the force back to the value of 18 nN the retracing path is curved before tip is separated from the sample. The force versus distance curve obtained after high load indentation does not match with the curve obtained before high load indentation [see Figs. 13(a) and (c)]. The curve after indentation can be fitted with two different values of slopes as indicated in the Fig. 13(c). Additional change in slope during unloading at lower loads may arise from the film material getting stuck and not letting the tip to separate.

III.5 Macroscale Friction and Wear Studies

For comparison, macroscale friction and wear measurements were performed using a ball-on-flat tribometer under reciprocating mode. Alumina ball with 6-mm diameter and surface roughness of about 3 nm rms was fixed in a stationary holder, and the coated samples were mounted on a reciprocating table. The normal load was applied by placing the dead weights on top of the ball holder. The friction force was measured with a strain gage ring. Initial coefficient of friction values are presented in Table 2. The

coefficient of friction as a function of sliding distance (or time) data are presented in Fig.14. A significant increase in the coefficient of friction during sliding suggests that the interface has degraded. Inflection point in the friction curves was taken as end of life.

We note that the coefficient of friction and durabilities of C_{18} double grafted film are superior to that of C_{18} single grafted film (Zarrad et al., 1993). ODT film exhibits slightly longer durability than that of ZnA film. C_{18} double grafted film exhibits lowest coefficient of friction and longest durability as compared to C_{18} single grafted, ZnA and ODT films. Trends in microscale friction and wear data are similar to that in microscale data.

IV. CONCLUSIONS

The atomic force and friction force microscopies have been successfully used to study the microtribological performance of SiO_2, C_{18} single and double grafted, Au, ODT and L-B films. The grafted films are uniform and devoid of holes. C_{18} double grafted film shows the lowest coefficient of friction value as compared to other samples measured in this study. Correlation between surface roughness and surface slope with friction force profile is very poor. This suggests that the topographic contribution to friction is small and local changes in friction force mostly occur because of the local changes on the film surface. The wear resistance of C_{18} double grafted film is much better than the SiO_2, C_{18} single grafted and L-B films. The C_{18} grafted films can withstand much higher normal force as compared to the L-B films. The coefficient of friction value for L-B film is comparable to the ODT layer and lower as compared to the Au film. The wear resistance of the L-B film is very poor and the wear initiates at the defects such as holes even at the normal force of about 100 nN. The nanoindentation studies show that the C_{18} double grafted films are much more rigid than the L-B films. Trends in macroscale friction and wear of various films are similar to that of microscale

data. Based on this study, C_{18} double grafted films appear to be suitable for lubrication of microcomponents.

ACKNOWLEDGMENT

The L-B Films were produced in the laboratory of Prof. M. Caffrey of the Department of Chemistry at The Ohio State University. This research was supported in parts by the Department of Navy, Office of Chief of Naval Research. The content of the information does not necessarily reflect the position or the policy of the Government, and no official endorsement should be inferred.

REFERENCES

Ando, E., Goto, Y., Morimoto, K., Ariga, K. and Okahata, Y., "Frictional Properties of Monomolecular Layers of Silane Compounds", Thin Solid Films, 180, 1989, pp. 287-291.

Bhushan, B., Handbook of Micro/Nanotribology, CRC Press, Boca Raton, FL, 1995.

Bhushan, B. and Koinkar, V.N., "Tribological Studies of Silicon for Magnetic Recording Applications", J. Appl. Phys., 75(10), 1994, pp.5741-5746.

Bhushan, B. and Ruan, J., "Atomic-Scale Friction Measurements Using Friction Force Microscopy: Part II- Application to Magnetic Media", ASME Journal of Tribology, 116, 1994, pp. 389-396.

Bowden, F.P., and Tabor, D., The Friction and Lubrication in Solids, Part I, Clarendon Press, Oxford, 1950, pp. 180-190.

Burnham, N.A., Colton, R.J. and Pollock, H.M., "Interpretation of Force Curves in Force Microscopy", Nanotechnology, 4, 1993, pp. 64-80.

Dean, J.A., Lange's Handbook of Chemistry, Mc Graw Hill, New York, 1979.

Duvault, Y., Gagnaire, A., Gardies, F., Jaffrezic-Renault, N., Martelet, C., Morel, D., Serpinet, J., Duvault, J.L, "Physicochemical Characterization of Covalently Bonded Alkyl Monolayer on Silica Surfaces", Thin Solid Films, 185, 1990, pp. 169-179.

Fan, L.S., Tai, Y.C. and Muller, R.S., Sensors and Actuators, 20, 1989, pp. 41.

Fujita, H., "Microtribology in Micro Machines", Japanese Journal of Tribology, 37, 1992, pp. 1375-1383.

Gabriel, K.J., Behi, F., Mahadevan, R., Mehregany, M., "In Situ Friction and Wear Measurement on Polysilicon Mechanisms", Sensors and Actuators, A21-A23, 1990, pp. 184-188.

Hansma, H.G., Gould, S.A.C., Hansma, P.K., Gaub, H.E., Longo, M.L., Zasadzinski, J.A.N., "Imaging Nanometer Defects in Langmuir-Blodgett Films with the AFM", Langmuir, 7, 1991, pp. 1051-1054.

Howe, R.T., "Surface Micromachining for Microsensors and Microactuators", J. Vac. Sci. Technol., B6(6), 1988, pp. 1809-1813.

Jaffrezic-Renault, N. and Martelet, C., "Preparation of Well-Engineered Thin Molecular Layer on Semiconductor-Based Transducers", Sensors and Actuators, A 32, 1992, pp. 307-312.

Liu, G.-Y. and Salmeron, M.B., "Reversible Displacement of Chemisorbed n-Alkanethiol Molecules on Au(111) Surface: An Atomic Force Microscope Study", Langmuir, 10, 1994, pp. 367-370.

Meyer, E. Overney, R., Luthi, R., Brodbeck, D., Howald, L., Frommer, F. and Guntherodt, H.J., Wolter, O., Fujihira, M., Takano, H. and Gotoh, Y., "Friction Force Microscopy of Mixed Langmuir-Blodgett Films", Thin Solid Films, 220, 1992, pp. 132-137.

Morel, D. and Serpinet, J., "Gas Chromatographic Evidence for Phase Transitions in Very Compact Octadecyl Bonded Silicas", J. Chromatography, 200, 1980, pp. 95-104.

O'Shea, S.J., Well and, M.E., Rayment, T., "An AFM Study of Grafted Polymers on Mica, Langmuir, 9, 1993, pp. 1826-1835.

Overney, R.M., Meyer, E., Frommer, J. and Guntherodt, H.J., "A Comparative Atomic Force Microscopic Study of Liquid Crystal Films: Transferred Freely-Suspended vs Langmuir-Blodgett. Morphology, Lattice and Manipulation", Langmuir, 9, 1993, pp. 341-346.

Overney, R.M., Takano, H., Fujihira, M., Meyer, E., and Guntherodt, H.J., "Wear, Friction and Sliding Speed Correlations on Langmuir-Blodgett Films Observed by Atomic Force Microscopy", Thin Solid Films, 240, 1994, pp. 105-109.

Pan, J., Tao, N., Lindsay, S.M., "An AFM Study of a Self Assembled Octadecyl Mercaptan Monolayer Adsorbed on Gold (111) Under Potential Control", Langmuir, 9, 1993, pp. 1556-1560.

Roberts, G.G., Langmuir-Blodgett Films, Plenum, NY, 1990.

Ruan, J.-A. and Bhushan, B., "Atomic-scale Friction Measurements using Friction Force Microscopy: Part I - General Principles and New Measurement Techniques", ASME Journal of Tribology, 116, 1994, pp. 378-388.

Ruhe, J. Novotny, V.J., Kanazawa, K.K., Clarke, T., and Street, G.B., "Structure and Tribological Properties of Ultrathin Alkylsilane Films Chemisorbed to Solid Surfaces", Langmuir, 9, 1993, pp. 2383-2388.

Schwartz, D.K., Viswanathan, R., Zasadzinski, J.A.N., "Coexisting Lattice Structures in a Langmuir-Blodgett Films Identified by AFM", Langmuir, 9, 1993, pp. 1384-1391.

Suzuki, S., Matsuura, T., Uchisawa, M., Yura, S., Shibata, H., "Friction and Wear Studies on Lubricants and Materials Applicable to MEMS", Tech. Digests, IEEE MEMS Workshop, 1991, pp. 143-147.

Suzuki, M., Saotome, Y., Yanagisawa, M., "Characterization of Monolayer and Bilayer Structures for Their Use as Lubricant", Thin Solid Films, 160, 1988, pp. 453-462.

Szabo, S., Le Ha, N., Schneider, P., Zeltner, P., Kovats, E. "Monofunctional (Dimethylamino) Silane as Silytating Agents", Helv. Chim. Acta, 67, 1984, pp. 2128-2142.

Tai, Y.C. and Muller, R.S., Sensors and Actuators, 20, 1989, pp. 49.

Ulman, A., An Introduction to Ultrathin Organic Films, Academic Press, Boston, 1991.

Viswanathan, R., Schwartz, D.K., Garnaes, J., Zasadzinski, J.A.N., "Atomic Force Microscopy Imaging of Substrate and pH Effects on Langmuir-Blodgett Monolayers", Langmuir, 8, 1992, pp. 1603-1607.

Wang, J., Caffrey, M., Bedzyk, M.J. and Penner, T.L., "Structure Changes in Model Membranes Monitored by Variable Period X-ray Standing Waves: Effect of Langmuir-Blodgett Film Thickness on Thermal Behavior", J. Phys. Chem. (in press).

Weisenhorn, A.L., Maivald, P., Butt, H.J. and Hansma, P.K., "Measurement of Adhesion, Attraction and Repulsion Between Surfaces in Liquids with an Atomic Force Microscope", Phys. Rev. B., 45(19), 1992, pp. 11226-11232.

Zarrad, H. Clechet, P., Belin, M., Martelet, C. and Jaffrezic-Renault, N., "The Use of Long-chain Molecules for Lubrication of Micromechanisms", J. Micromech. Microeng., 3, 1993, pp. 222-224.

Zasadzinski, J.A., Viswanathan, R., Madsen, L., Garnaes, J. and Schwartz, D.K., "Langmuir-Blodgett Films", Science, 263, 1994, pp. 1726-1733.

TABLE 1

Bond Energies of different molecules at 298 ^{o}K (Dean, 1979)

Bond	Bond Energy (kJ/mol)
Au-S	418
S-C	699
Si-O	798
Si-C	435

TABLE 2

Typical rms roughness and microscale and macroscale coefficients of friction values of various samples

Specimen	rms Roughness (nm)*	Microscale Coefficient of Friction**	Macroscale Coefficient of Friction***
Si(100)	0.12	0.03	0.18
SiO_2/Si	0.21	0.03	0.19
C_{18} single grafted/SiO_2/Si	0.16	0.04	0.23
C_{18} double grafted/SiO_2/Si	0.16	0.018	0.07
Au/Si	1.16	0.04	0.13
ODT/Au/Si	0.92	0.03	0.14
ZnA/ODT/Au/Si	0.55	0.03	0.16

* rms roughness measured on 1 μm x 1 μm scan area using AFM

** Si_3N_4 tip with a radius of about 30-50 nm at normal force in the range of 10-200 nN and scanning speed of 4 μm/s on a 1 μm x 1 μm scan area.

*** Alumina ball with 3-mm radius at normal loads of 0.1 N and average sliding speed of 0.8 mm/s

FIGURE CAPTIONS

Figure 1. Schematic of the Octodecyl (C_{18}) and docosyl (C_{22}) grafted film on silica.

Figure 2. Schematic of the zinc arachidate L-B film on ODT with a gold underlayer.

Figure 3. Gray scale plots of (a) SiO_2/Si [surface roughness (σ= 0.21 nm), slope of the surface along the sample sliding direction (mean =0.0, σ=0.12), and friction force (mean=3.10 nN, σ=0.77 nN), (b) C_{18} single grafted film [surface roughness (σ=0.16 nm), slope of the surface along the sample sliding direction (mean=0.0, σ=0.01), and friction force (mean=4.8 nN, σ=3.23 nN), and (c) C_{18} double grafted film [surface roughness (σ=0.16 nm), slope of the surface along the sample sliding direction (mean=0.0, σ=0.01), and friction force (mean=1.95 nN, σ=0.01 nN) for a total normal force (including external and intrinsic adhesive forces) of 110 nN.

Figure 4. Friction force as a function of normal force for SiO_2/Si, C_{18} single grafted and C_{18} double grafted films.

Figure 5. Gray scale plots of (a) Au/Si [surface roughness (σ= 1.16 nm), slope of the surface along the sample sliding direction (mean = 0.0, σ= 0.07), and friction force (mean=1.5 nN, σ=0.10 nN), (b) ODT/Au/Si [surface roughness (σ=0.92 nm), slope of the surface along the sample sliding direction (mean= 0.0, σ= 0.02), and friction force (mean=1.10 nN, σ=0.07 nN), and (c) ZnA/ODT/Au/Si [surface roughness (σ=0.55 nm), slope of the surface along the sample sliding direction (mean=0.0, σ=0.023), and friction force (mean=1.1 nN, σ=3.24 nN) for a total normal force of 40 nN.

Figure 6. Friction force as a function of normal force for Au/Si, ODT/Au/Si and ZnA/ODT/Au/Si.

Figure 7. Topographic images of C_{18} double grafted film (2 nm x 2 nm) and corresponding fourier transform spectrum at two normal forces.

Figure 8. (a) Gray scale friction plots of ZnA films at total normal force of 200 nN and different numbers of scan cycles. Number of scan cycles are indicated in figure and (b) central region of 1 μm x 1 μm imaged at normal force of 40

nN, shows the worn region of ZnA/ODT/Au/Si after four scan cycles and 2-D section shows the steps of approximately 6.5 nm with debris collected at the edges of wear track.

Figure 9. (a) Wear depth as a function of normal force after one scan cycle (b) Wear depth as a function of number of scan cycles at the normal force indicated for SiO_2/Si, C_{18} single grafted, C_{18} double grafted, Au/Si, ODT/Au/Si and ZnA/ODT/Au/Si.

Figure 10. Surface profiles showing the worn region (center 1 μm x 1 μm) after one scan cycle for SiO_2/Si, C_{18} single grafted, C_{18} double grafted, Au/Si, ODT/Au/Si and ZnA/ODT/Au/Si. Normal force and the wear depth are indicated in the figure.

Figure 11. Surface profiles of C_{18} double grafted film showing the worn region (center 1 μm x 1 μm) .The normal load, wear depth and number of scan cycles are indicated in the figure.

Figure 12. Cantilever force versus sample traveling distance curves obtained at force of 18 nN for (a) Silicon (100), (b) C_{18} double grafted layer and (c) ZnA/ODT/Au/Si film. The arrows in the figure indicates the sample traveling direction. Slopes of curves are given in the figure.

Figure 13. Cantilever force versus sample traveling distance curves for ZnA/ODT/Au/Si film at indentation force of (a) 18 nN, (b) 32.4 nN and (c) 18 nN. The arrows in the figure indicates the sample traveling direction. Slopes of curves are given in the figure.

Figure 14. Coefficient of friction as a function of sliding distance for a 3-mm radius alumina ball rubbing against (a) Silicon (100), SiO_2/Si, C_{18} single grafted, and C_{18} double grafted layer, and (b) Au/Si, ODT/Au/Si and ZnA/ODT/Au/Si films. Test conditions were : Normal load = 0.1 N, average sliding speed = 0.8 mm/s, temperature = 22 $\pm$ 1°C and relative humidity = 45 $\pm$ 5%.

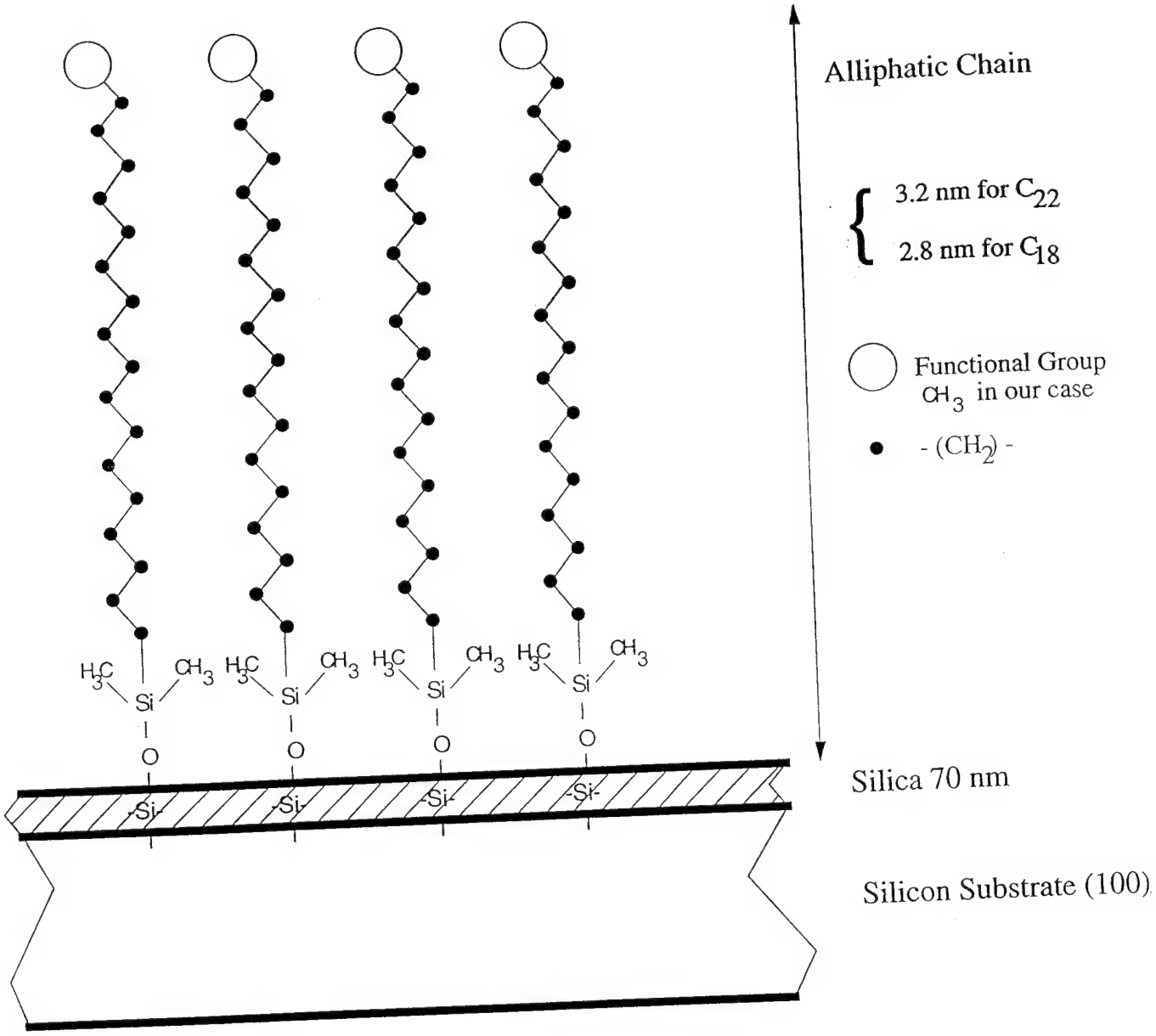
Alliphatic Chain
3.2 nm for C_{22}
2.8 nm for C_{18}
Functional Group
CH_3 in our case
- (CH_2) -
Silica 70 nm
Silicon Substrate (100)

Fig. 1

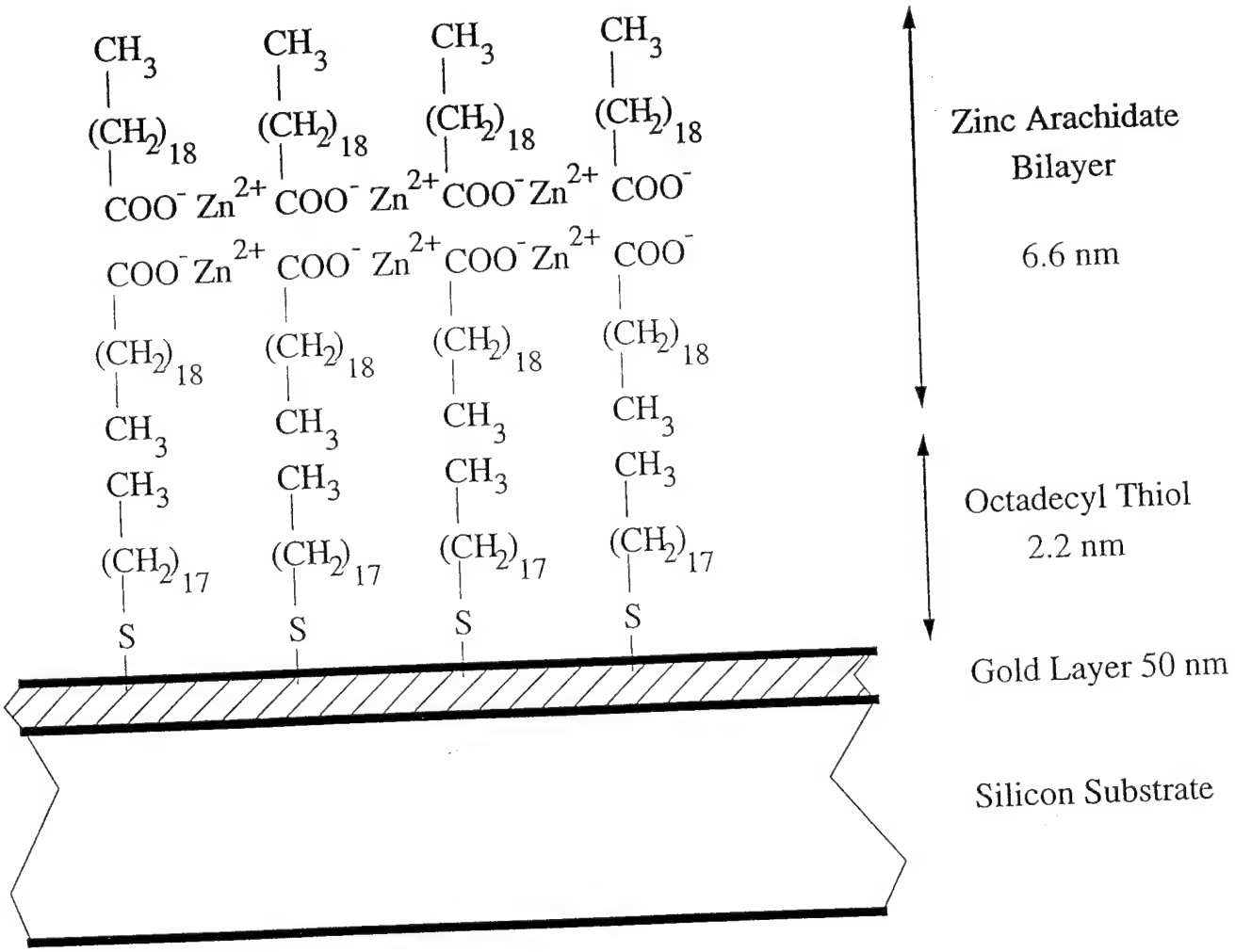
Zinc Arachidate
Bilayer
6.6 nm
Octadecyl Thiol
2.2 nm
Gold Layer 50 nm
Silicon Substrate

Fig. 2

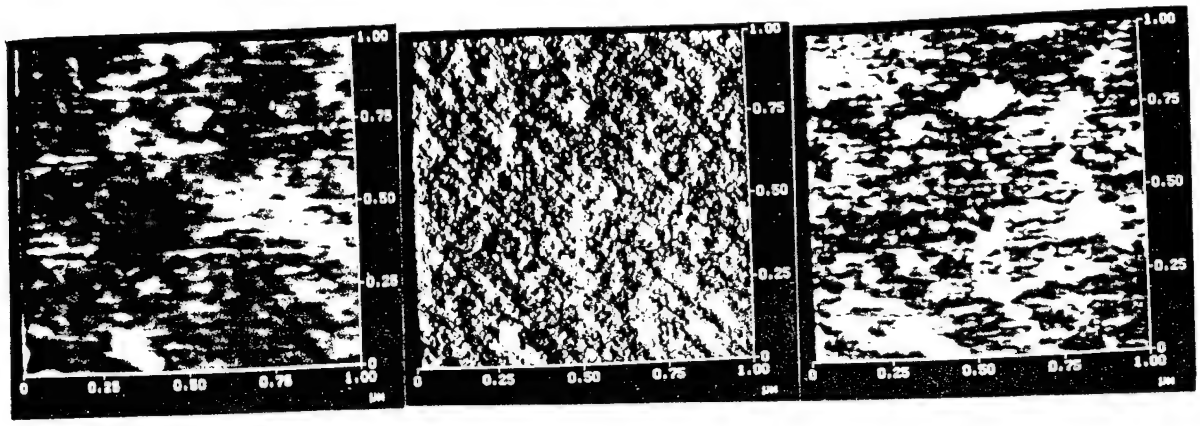

(a) SiO_2/Si

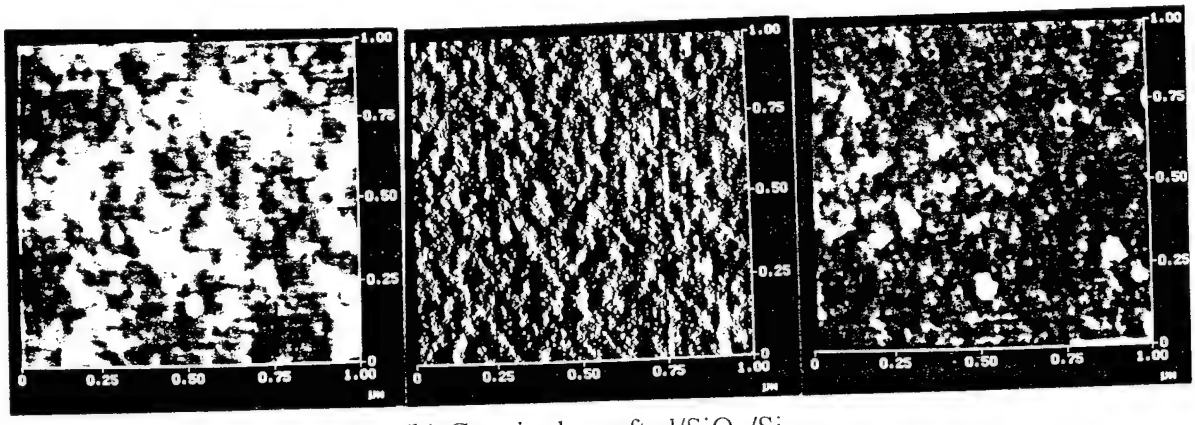

(b) C_{18} single grafted/SiO_2/Si

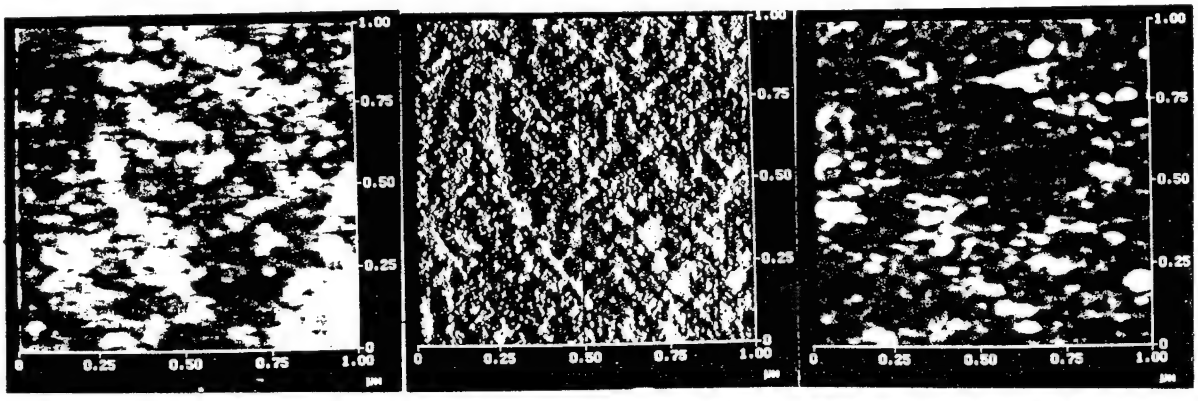

(c) C_{18} double grafted/SiO_2/Si

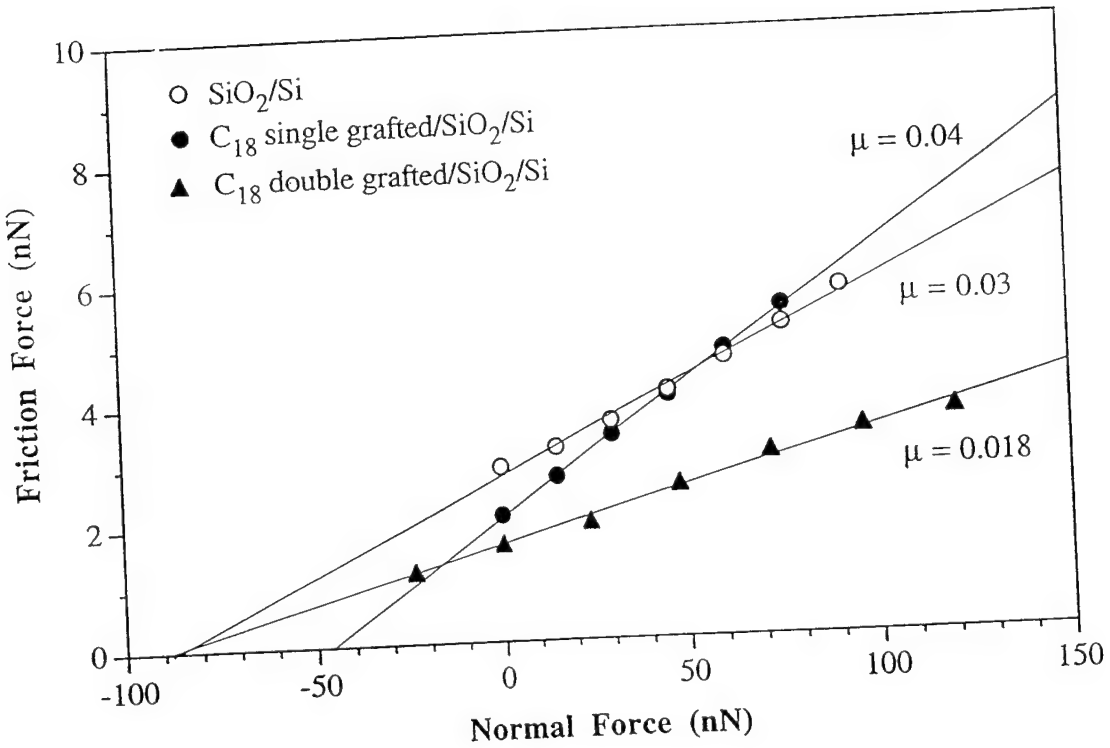
10
8
6
4
2
0
-100
-50
0
50
100
150
Friction Force (nN)
Normal Force (nN)
○ SiO_2/Si
● C_{18} single grafted/SiO_2/Si
▲ C_{18} double grafted/SiO_2/Si
μ = 0.04
μ = 0.03
μ = 0.018

Fig.4

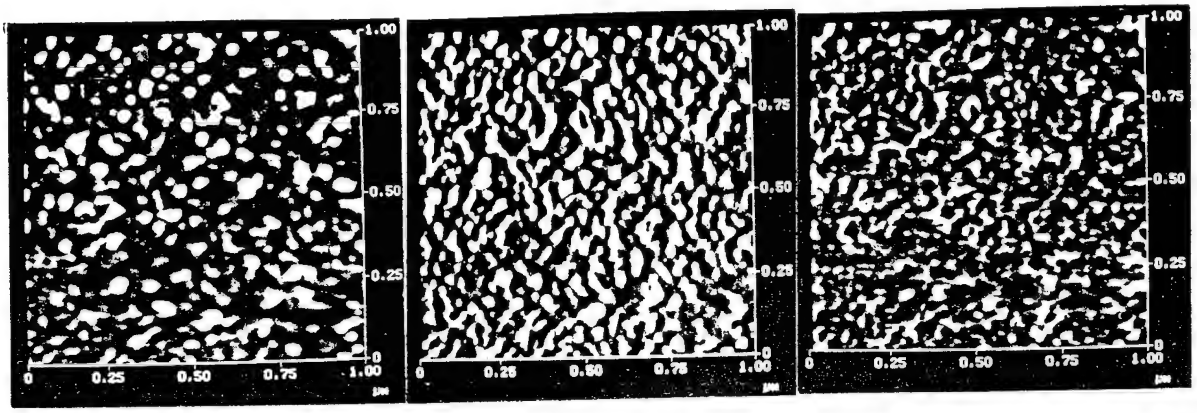

(a) Au/Si

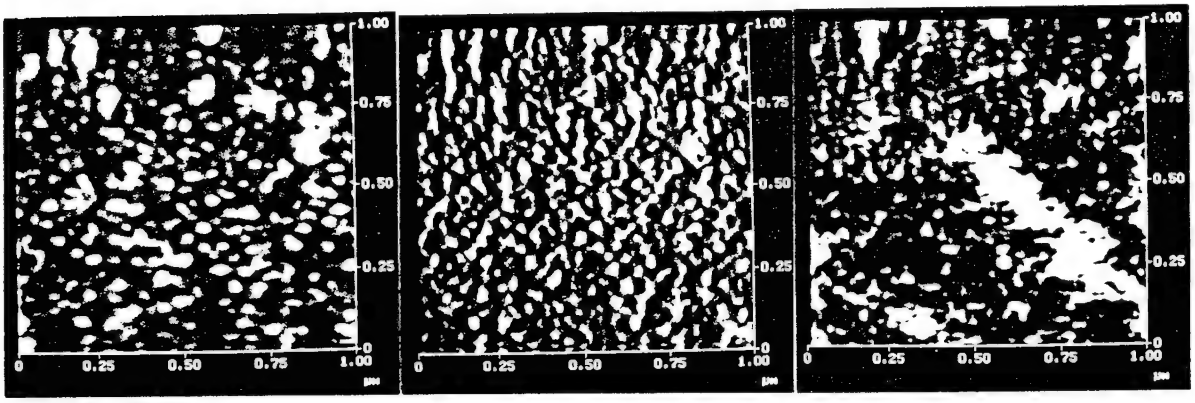

(b) ODT/Au/Si

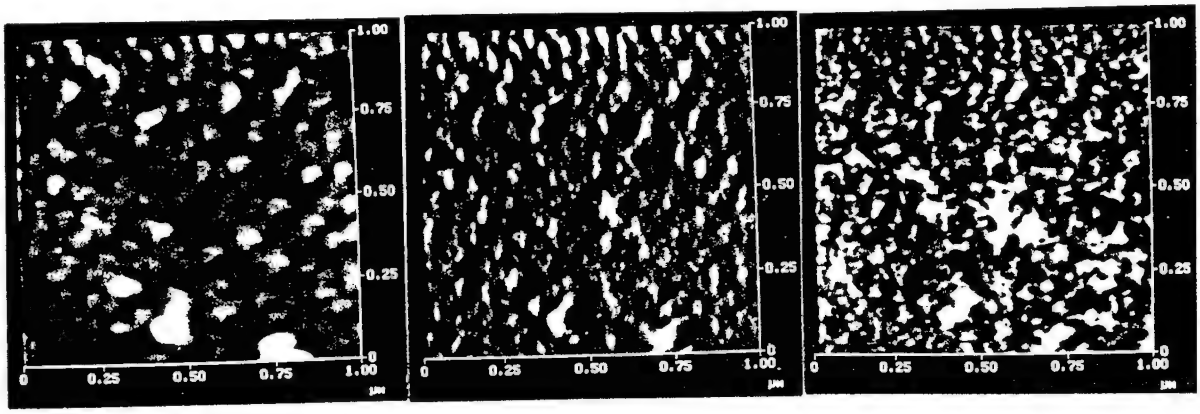

(c) ZnA/ODT/Au/Si

Fig. 5

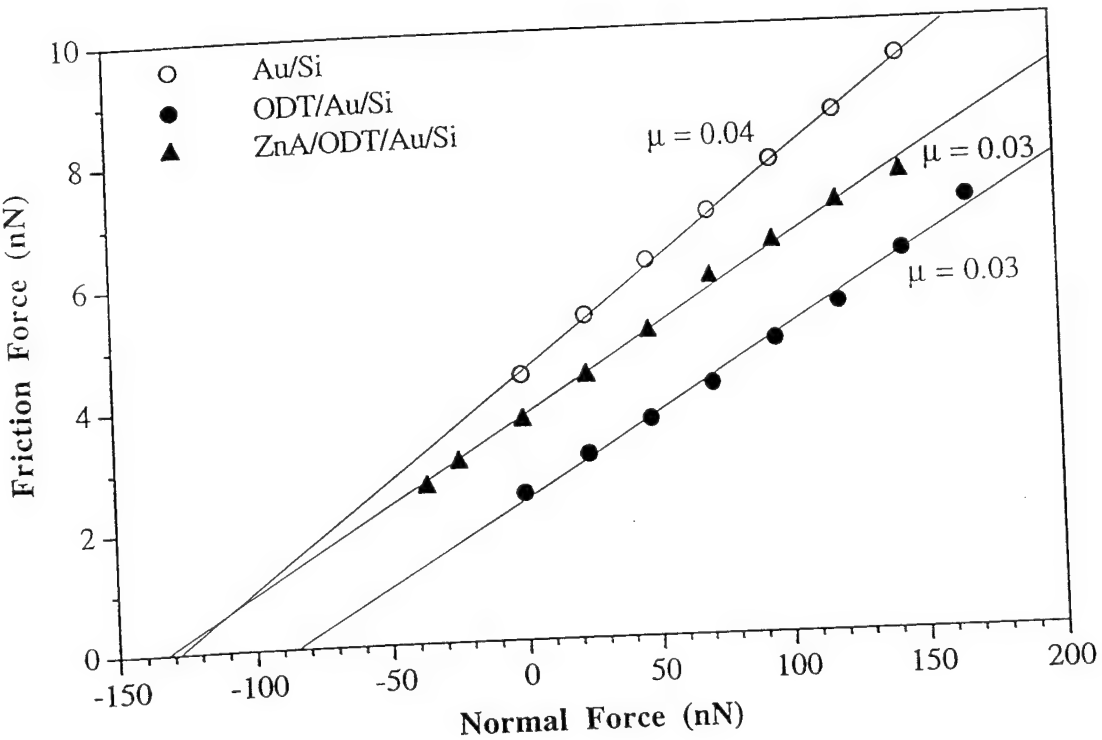
Au/Si
ODT/Au/Si
ZnA/ODT/Au/Si
μ = 0.04
μ = 0.03
μ = 0.03
Friction Force (nN)
Normal Force (nN)
10
8
6
4
2
0
-150
-100
-50
0
50
100
150
200

Fig. 6

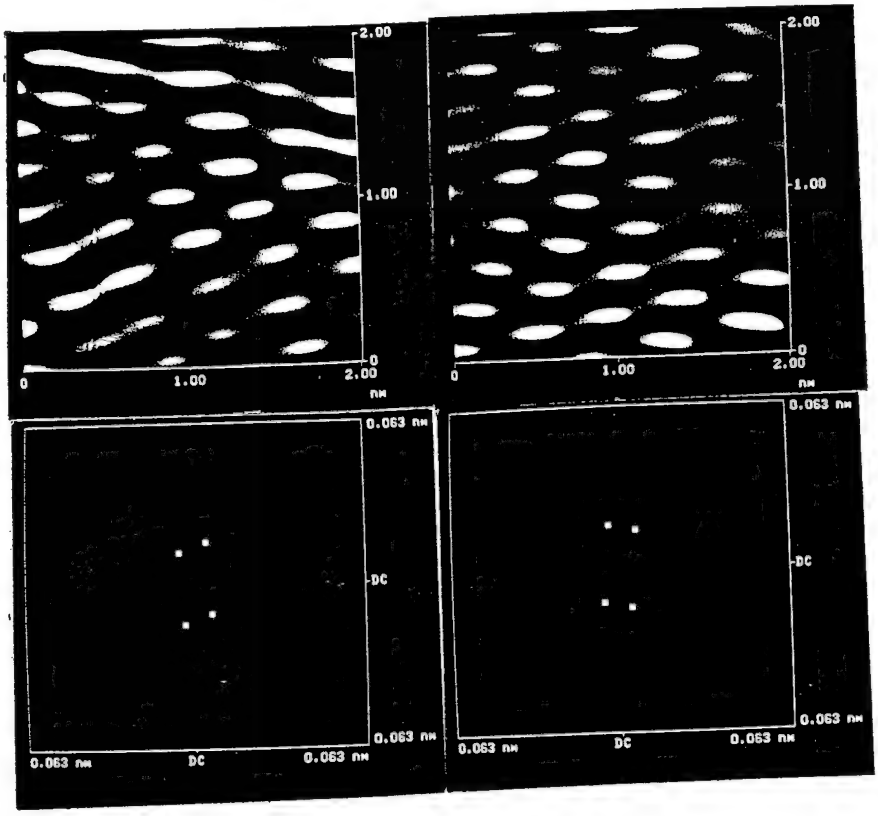

40 nN

250 nN

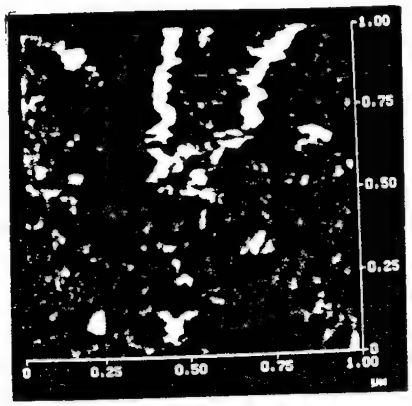

After first cycle

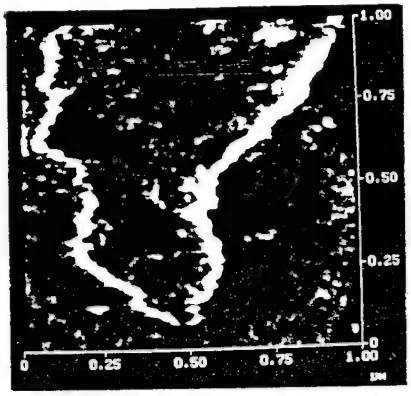

After second cycle

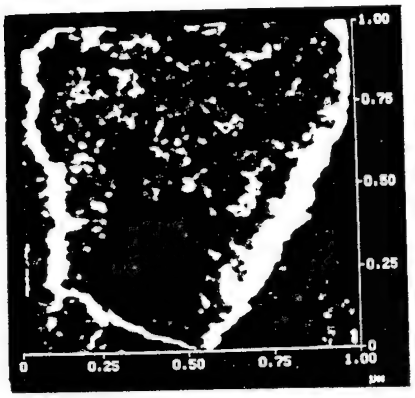

After third cycle

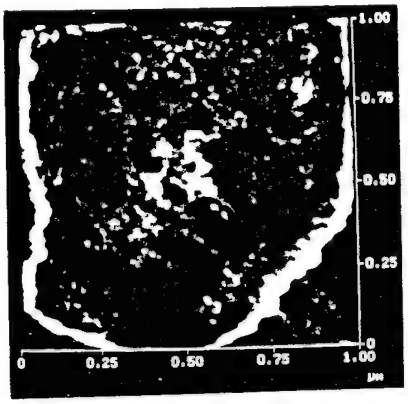

After fourth cycle

(a)

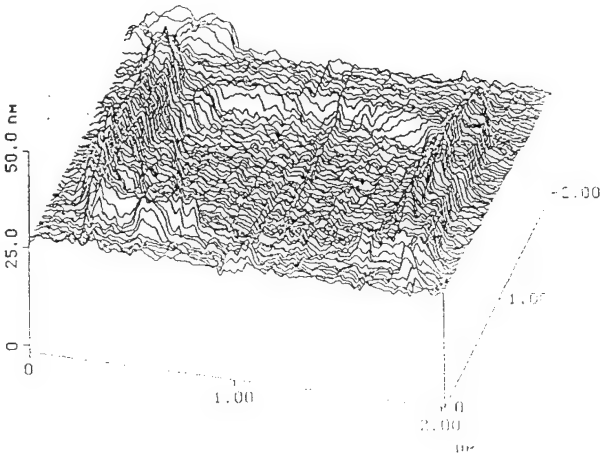

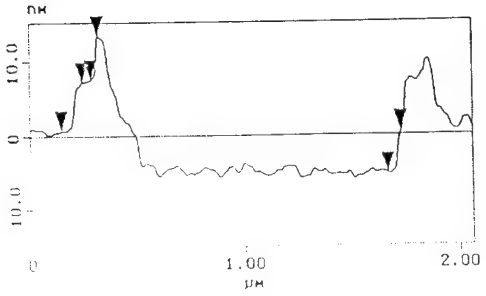

(b)

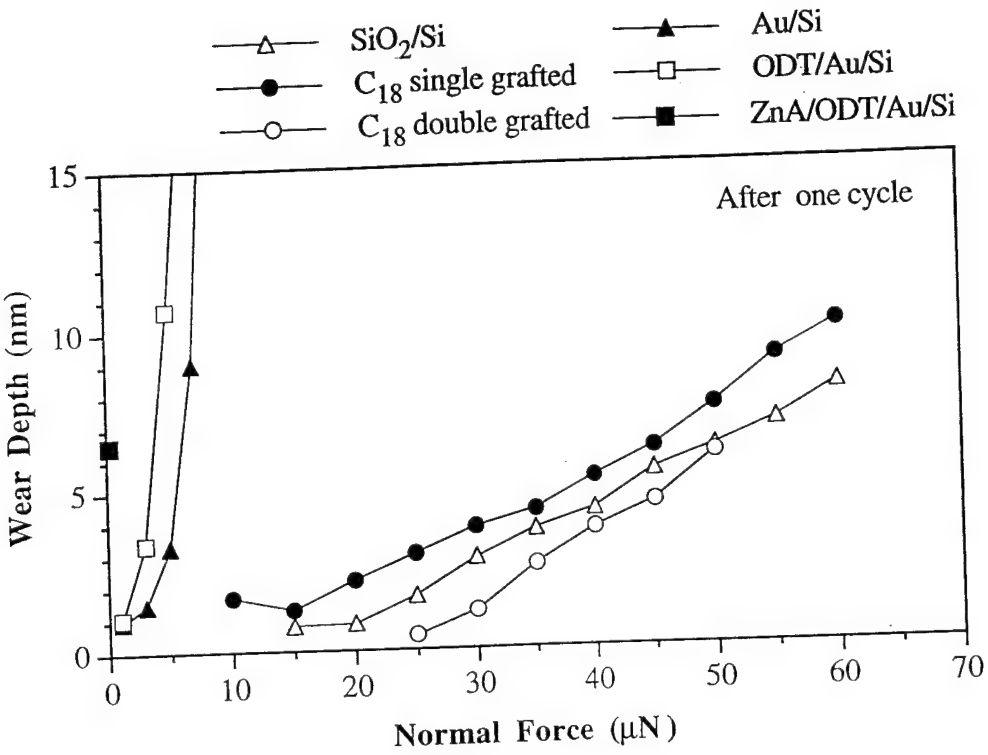
SiO_2/Si
C_{18} single grafted
C_{18} double grafted
Au/Si
ODT/Au/Si
ZnA/ODT/Au/Si
After one cycle
Wear Depth (nm)
Normal Force (μN)
0
5
10
15
0
10
20
30
40
50
60
70

(a)

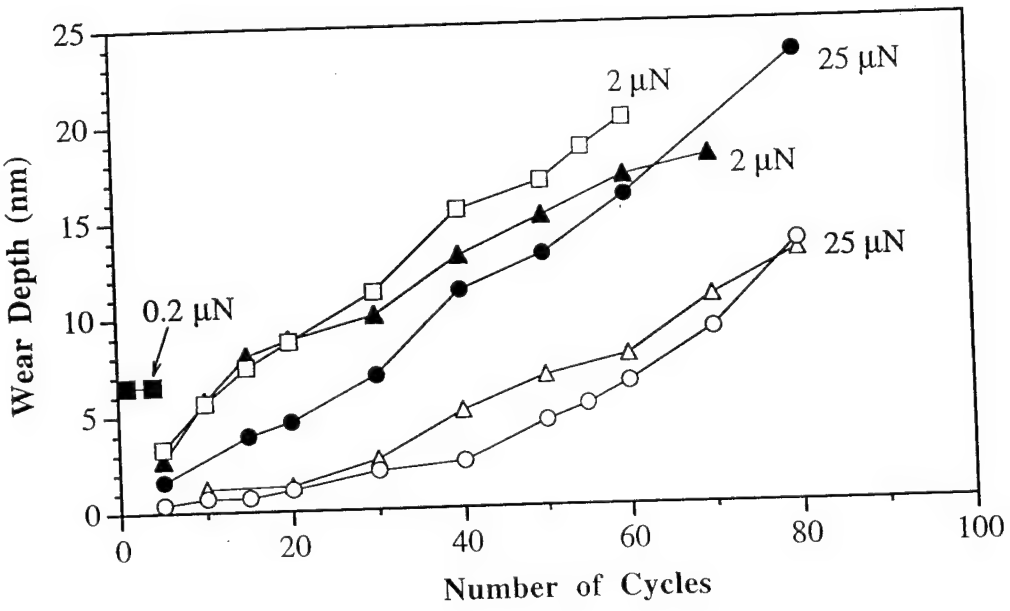
2 μN
25 μN
2 μN
25 μN
0.2 μN
Wear Depth (nm)
Number of Cycles
0
5
10
15
20
25
0
20
40
60
80
100

(b)

Fig. 9

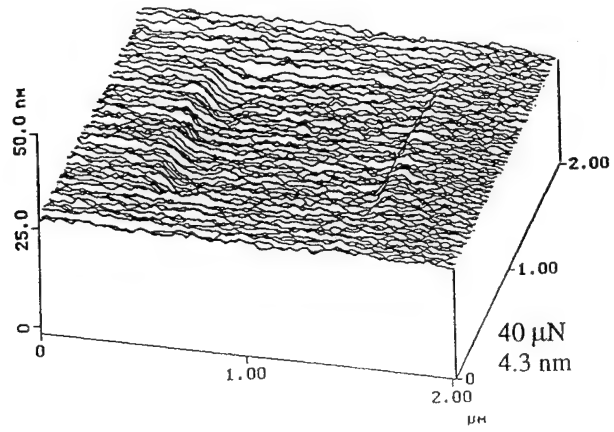

SiO_2/Si

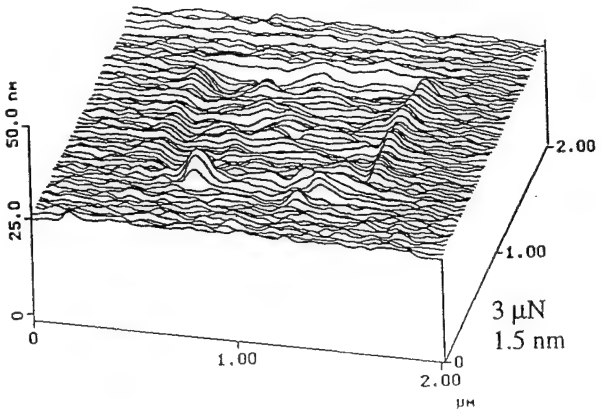

Au/Si

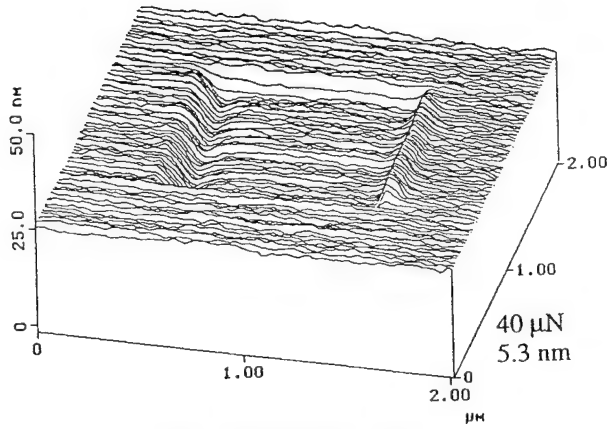

C_{18} single grafted/SiO_2/Si

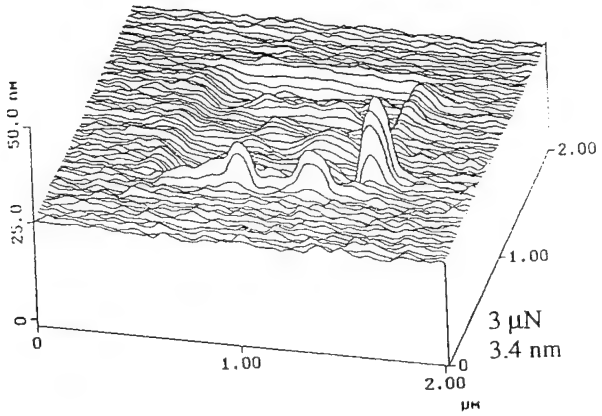

ODT/Au/Si

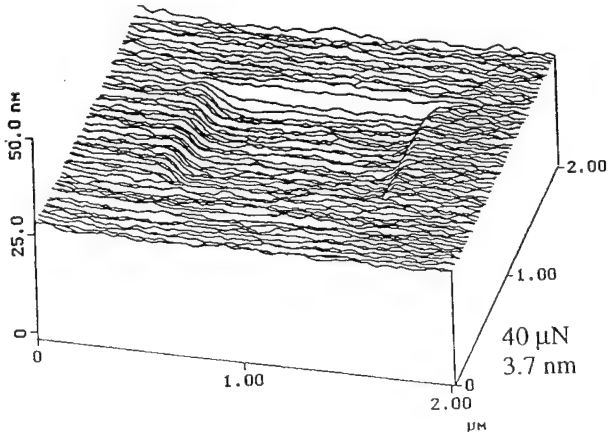

C_{18} double grafted/SiO_2/Si

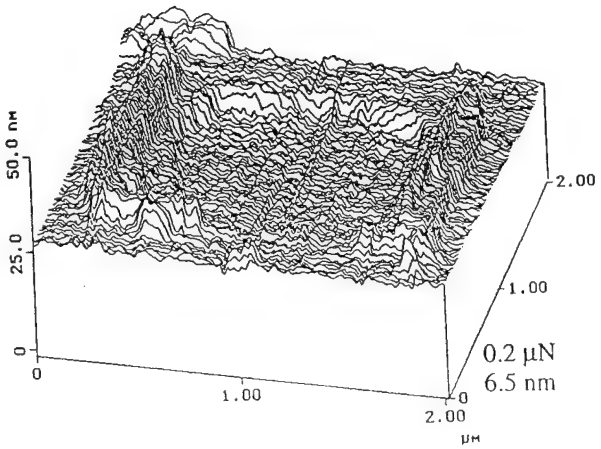

ZnA/ODT/Au/Si

Fig 10

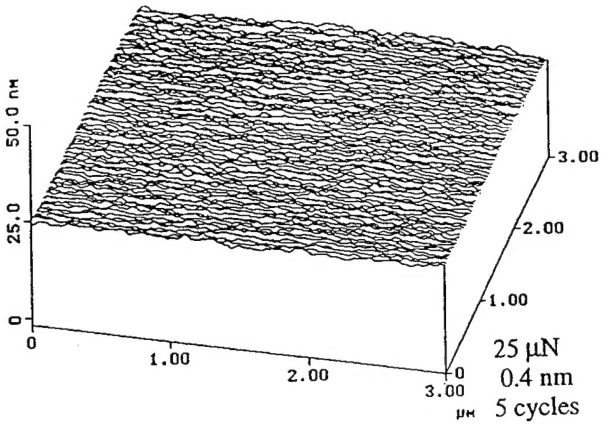
50.0 nm
25.0
0
0
1.00
2.00
3.00
μm
3.00
2.00
1.00
0
25 μN
0.4 nm
5 cycles

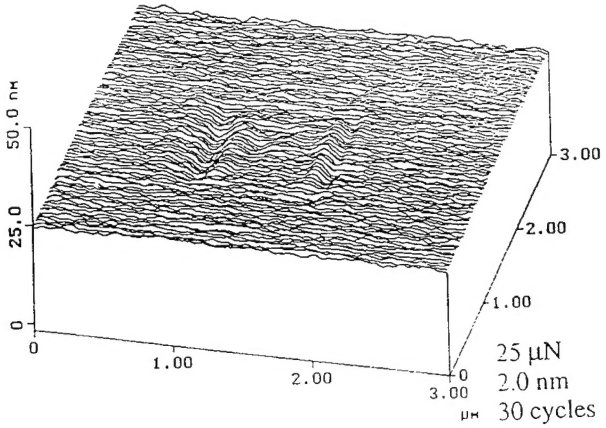
50.0 nm
25.0
0
0
1.00
2.00
3.00
μm
3.00
2.00
1.00
0
25 μN
2.0 nm
30 cycles

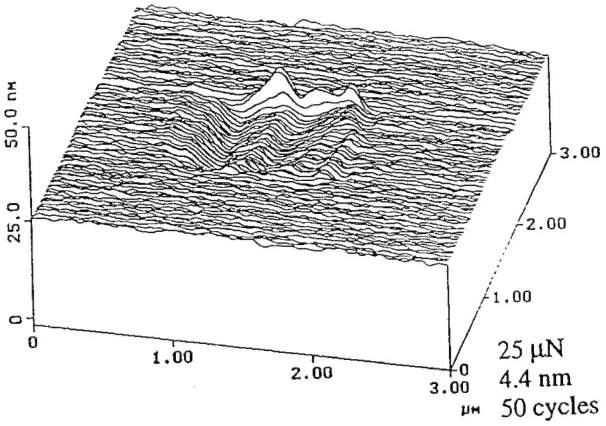
50.0 nm
25.0
0
0
1.00
2.00
3.00
μm
3.00
2.00
1.00
0
25 μN
4.4 nm
50 cycles

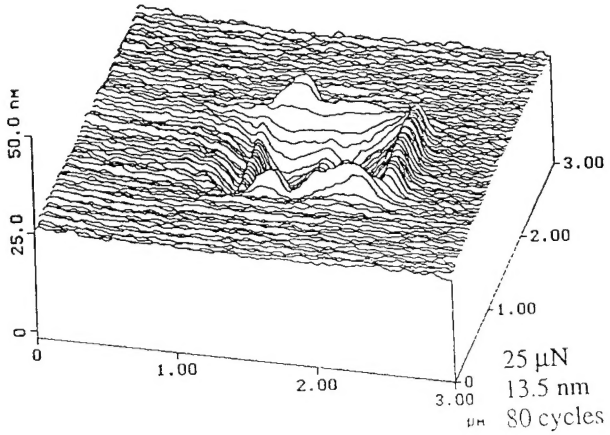
50.0 nm
25.0
0
0
1.00
2.00
3.00
μm
3.00
2.00
1.00
0
25 μN
13.5 nm
80 cycles

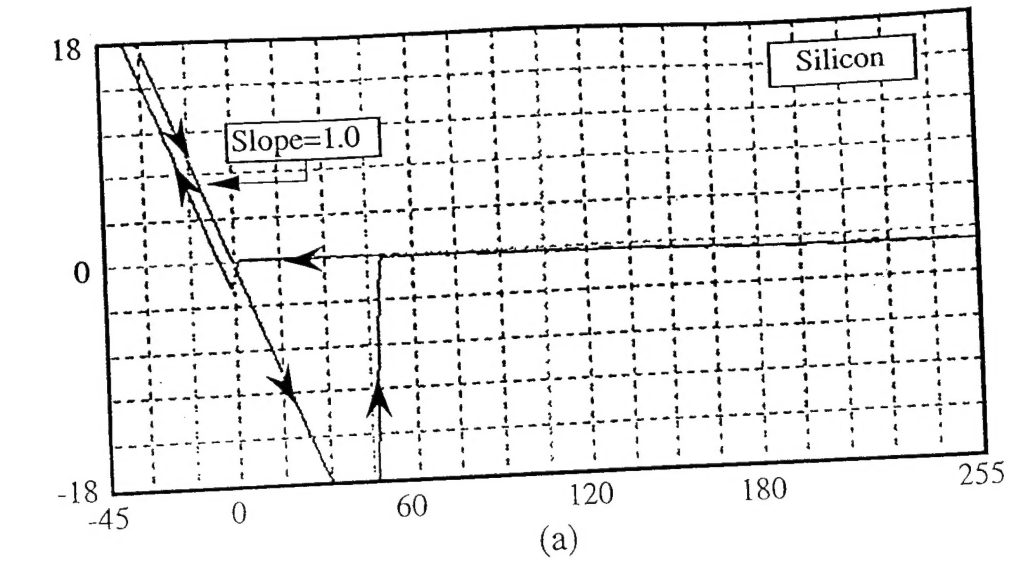
Silicon
Slope=1.0
18
0
-18
-45
0
60
120
180
255

(a)

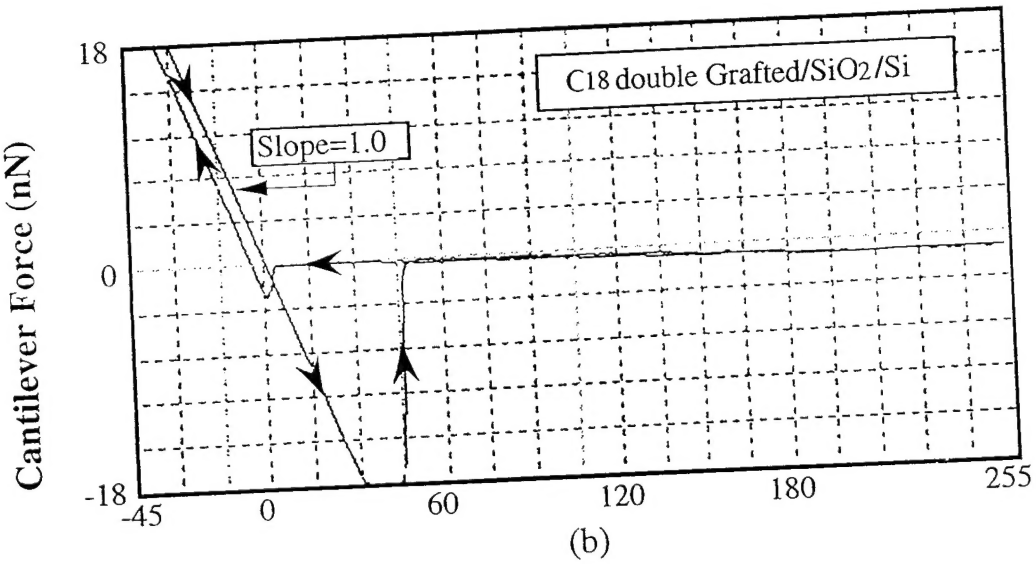
C18 double Grafted/SiO2/Si
Slope=1.0
18
0
-18
-45
0
60
120
180
255

(b)

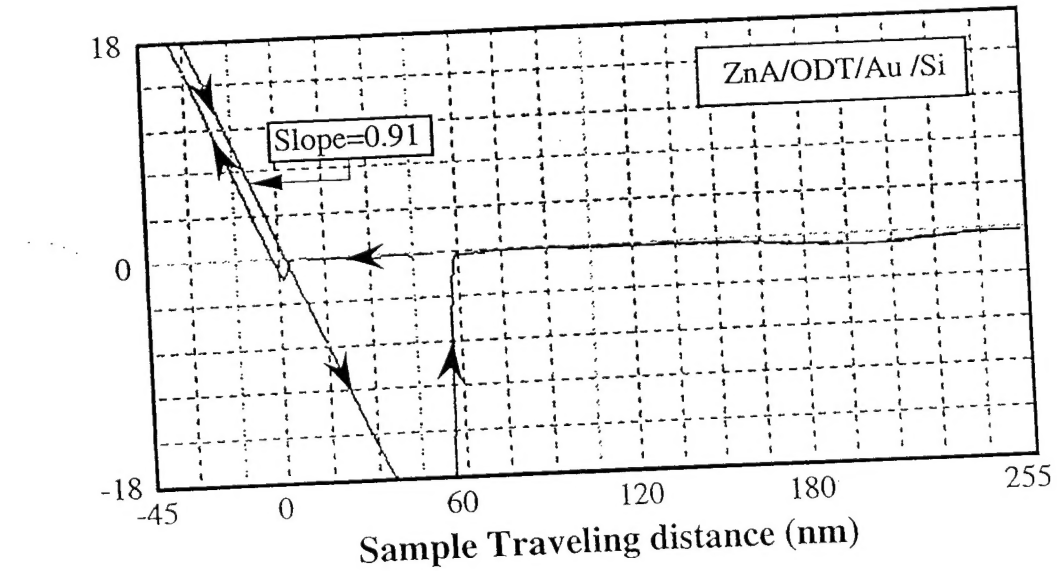
ZnA/ODT/Au /Si
Slope=0.91
18
0
-18
-45
0
60
120
180
255
Cantilever Force (nN)
Sample Traveling distance (nm)

(c)

Fig. 12

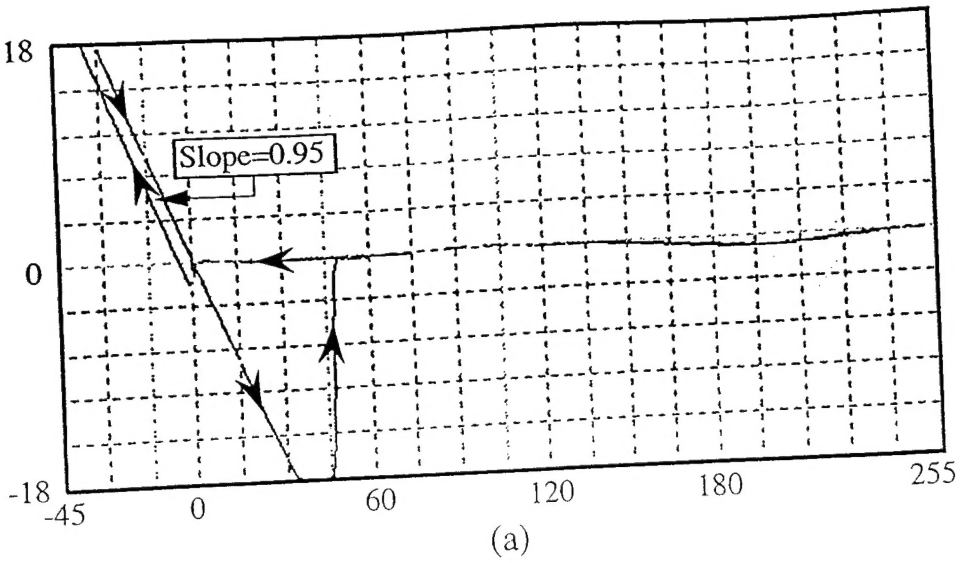
18
0
-18
Slope=0.95
-45
0
60
120
180
255

(a)

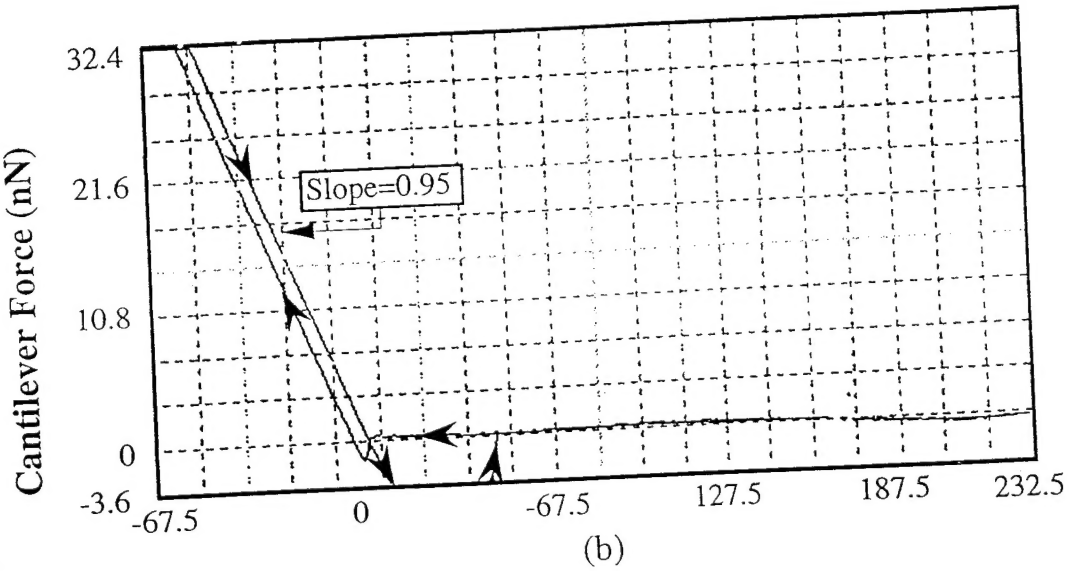
Cantilever Force (nN)
32.4
21.6
10.8
0
-3.6
Slope=0.95
-67.5
0
-67.5
127.5
187.5
232.5

(b)

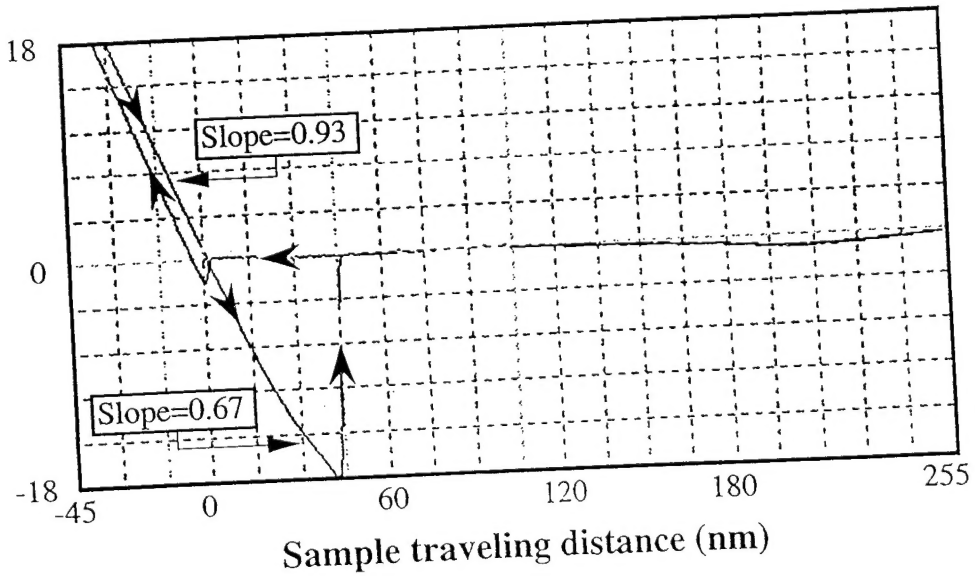
18
0
-18
Slope=0.93
Slope=0.67
-45
0
60
120
180
255
Sample traveling distance (nm)

(c)

Fig. 13

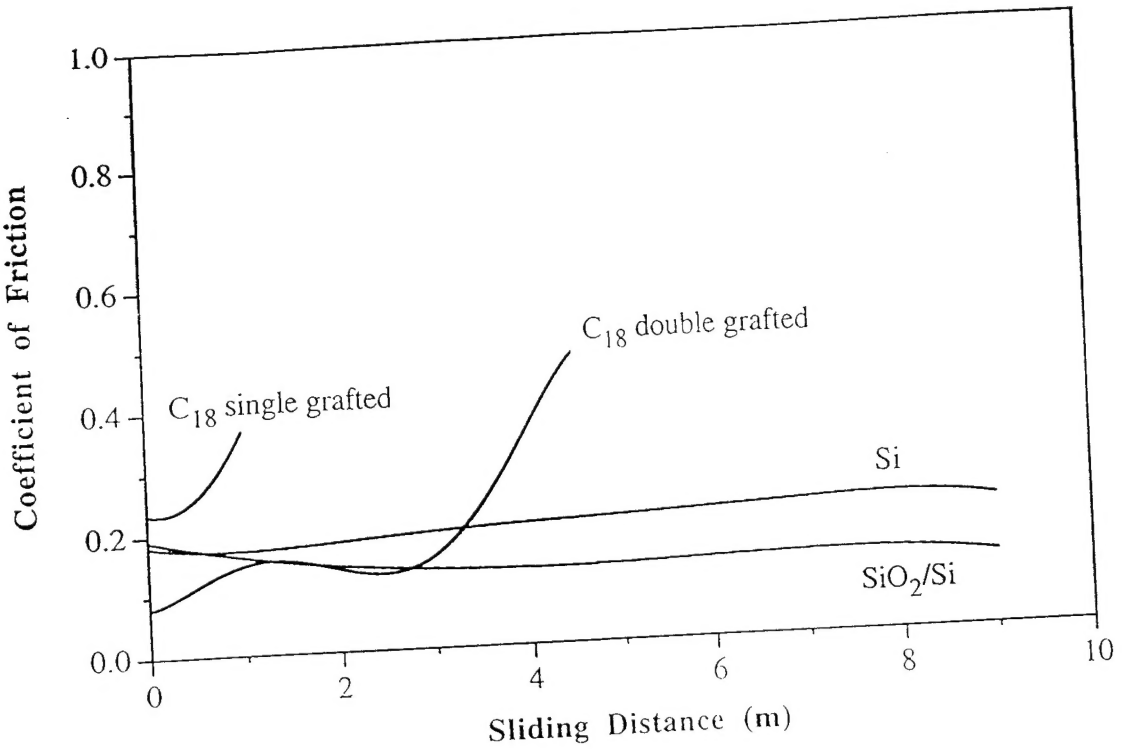
Coefficient of Friction
1.0
0.8
0.6
0.4
0.2
0.0
0
2
4
6
8
10
Sliding Distance (m)
C_{18} single grafted
C_{18} double grafted
Si
SiO_2/Si

(a)

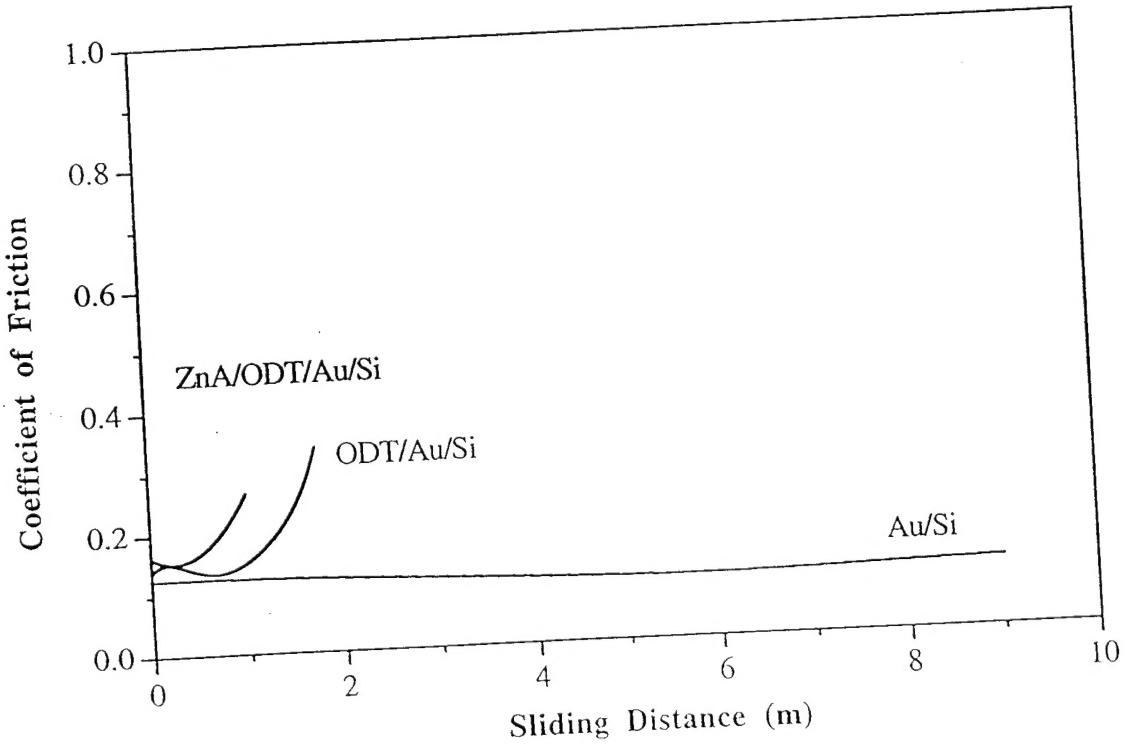
Coefficient of Friction
1.0
0.8
0.6
0.4
0.2
0.0
0
2
4
6
8
10
Sliding Distance (m)
ZnA/ODT/Au/Si
ODT/Au/Si
Au/Si

(b)

Fig. 14